Molecular Crystals and Liquid Crystals
Publication details, including instructions for authors and subscription information:
http://www.tandfonline.com/loi/gmcl16

Homogeneous Instability under Free Convection in a Tilted Nematic Sample

U. D. Kini [a]
[a] Raman Research Institute, Bangalore, 560 080, India

Version of record first published: 17 Oct 2011.

To cite this article: U. D. Kini (1983): Homogeneous Instability under Free Convection in a Tilted Nematic Sample, Molecular Crystals and Liquid Crystals, 99:1, 223-237

To link to this article: http://dx.doi.org/10.1080/00268948308072044

Mol. Cryst. Liq. Cryst., 1983, Vol. 99, pp. 223–237
0026-8941/83/9904–0223/$18.50/0

Printed in the United States of America

Homogeneous Instability under Free Convection in a Tilted Nematic Sample†

U. D. KINI

Raman Research Institute, Bangalore 560 080, India

(Received January 11, 1983; in final form April 20, 1983)

Exact calculations on homogeneous instability (HI) threshold under free convection in a tilted nematic sample are presented. Inclusion of the effect of secondary flow leads to HI threshold value in close agreement with the experimental result for MBBA. Effects of stabilizing and destabilizing magnetic fields on the HI threshold are studied. Calculations are extended to HBAB where it is shown that under the joint action of the stabilizing effect of free convection and the destabilizing effect of magnetic field, HI may occur in the sample. At high enough values of destabilizing field it may be possible to observe a mode (involving net secondary flow) of HI which is generally unfavorable. The presence of secondary flow may lead to a loss of scaling for materials which show a divergence of twist viscosity near the nematic–smectic A transition.

I. INTRODUCTION

Though thermal instabilities in nematic liquid crystals have been investigated in detail both experimentally and theoretically,[1] not much work appears to have been done on free convection. The first effort in this direction appears to be that of Horn *et al.*[2] who studied the effect of free convection in tilted nematic samples containing different initial alignment of director. In particular they found that when the director is initially aligned normal to the shear plane a homogeneous instability (HI, similar to that observed in Ref. 3) occurs above a threshold shear rate which is determined by a threshold temperature difference $(\Delta T)_c$ between the plates

†Presented at the Ninth International Liquid Crystal Conference, Bangalore, December 1982.

of the tilted sample. They further showed on the basis of a simple model, ignoring transverse flow that the HI threshold obeys a scaling law $d^3 (\Delta T)_c \cos \psi =$ constant for a given material, where d is the sample thickness and ψ the angle of tilt of the plates with the vertical. More recently Guyon *et al.*[4] showed that in a nearly horizontal sample free convection can modulate the size of convection rolls making alternate rolls larger.

In this communication an exact calculation is presented for HI threshold in a tilted nematic sample for the case studied in Ref. 2. For MBBA the exact results are in close quantitative agreement with the experimental result of Ref. 2. Calculations are extended to HBAB for which HI is shown to be possible under the combined action of stabilizing shear and destabilizing magnetic field whose strength exceeds Freedericksz threshold. For sufficiently strong destabilizing fields it may be possible to observe a mode of HI involving net transverse flow provided that a convective instability is not more favorable.

2. ASSUMPTIONS, DIFFERENTIAL EQUATIONS AND MODAL ANALYSIS

Calculations essentially follow Ref. 2 and are based on the Ericksen-Leslie continuum theory of incompressible uniaxial nematics having constant director magnitude.[5] The nematic with director orientation $\mathbf{n}_0 = (1, 0, 0)$ is confined between plates $z = \pm d/2$ which are maintained at temperatures T_2 and T_1 respectively. To fix ideas, let $\Delta T = T_1 - T_2 > 0$. The y axis makes an angle ψ with the vertical (Figure 1). The uncompensated buoyancy force along y causes free convection to set in even for very small temperature differences since the characteristic length along y, the length of the plates $\sim$ a few cm $\gg d$ the sample thickness. Free convection sets in essentially as a roll with axis along x and wavelength $\sim$ sample length. However, far from sample edges all quantities associted with flow can be assumed to vary with z. With $\mathbf{n}_0 = (1, 0, 0)$ the velocity $v = (0, v_{y0}(z), 0)$, temperature $T_0(z)$ and pressure $p_0(z)$ are given by

$$\frac{1}{2} \mu_4 \, v_{y0,zz} - \rho\beta \, g_y \, T_v = 0 \tag{1}$$

$$k_1 \, T_{0,zz} + \left[\frac{1}{2} \mu_4 \, v_{y0,z}^2\right] = 0 \tag{2}$$

$$p_{0,z} + \rho g_z \, \beta \, T_v = 0 \tag{3}$$

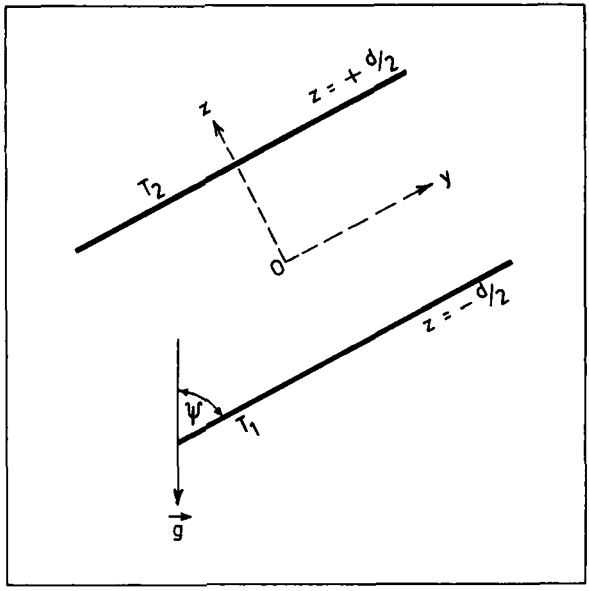

FIGURE 1 Sample configuration. Sample thickness $d \ll$ linear dimensions of plates $z = \pm d/2$, which are so tilted that y axis makes an angle ψ with the vertical or an angle $\pi - \psi$ with **g**, the acceleration due to gravity. Initial director orientation is along x, out of the figure plane. Plates $z = \pm d/2$ are maintained at temperatures T_2 and T_1 respectively. Free convection sets in as a flow $v_{y0}(z)$ in the yz plane, far away from sample edges. For $\Delta T = T_1 - T_2 > 0$ steady state fluid flow is along $+y(-y)$ in the region $z < 0$ ($z > 0$).

where μ_4 is a viscosity coefficient, ρ the density, $\mathbf{g} = [0, -g \cos \psi - g \sin \psi]$ the acceleration due to gravity, β the thermal expansion coefficient, k_1 the thermal conductivity normal to the director, $T_v = T_0(z) - (T_1 + T_2)/2$ the excess temperature at a point z over the mean[6] and $p_{0,z} = dp_0/dz$, etc. In principle one has to solve Eqs. (1)–(3) subject to boundary conditions

$$T_v(\pm d/2) = \mp(\Delta T)/2, \qquad v_{y0}(\pm d/2) = 0 \tag{4}$$

If T_v is known, p_0 can be determined from Eq. (3) to within an arbitrary constant. Exact computation shows that for sufficiently small values of ΔT, $T_0(z)$ is linear in z. Hence, for simplicity the term [ ] in Eq. (2) is ignored. Then with $T_v = -(\Delta T)z/d$ one finds from Eqs. (1) and (4) that

$$v_{y0}(z) = \overline{G}(z^3 - zd^2/4)$$
$$\overline{G} = \rho g \beta (\Delta T)(\cos \psi)/3\mu_4 d \tag{5}$$

Let homogeneous perturbations (which are functions of z and time t alone) be impressed on velocity, director, temperature and pressure. Then

$$\mathbf{v} = [v_x'(z,t), v_{y0}(z) + v_y'(z,t), 0];$$

$$\mathbf{n} = [1, \varphi(z,t), \theta(z,t)];$$

$$T(z,t) = T_0(z) + T'(z,t);$$

$$p(z,t) = p_0(z) + p'(z,t).$$

The temperature difference ΔT and angle ψ are assumed to be sufficiently small so that convective instability is not favored. Also effects of lateral dimensions of the sample are not considered.

The torque, force and thermal conduction equations when linearized with respect to fluctuations ψ, θ, v_x', v_y', p' and T' become

$$\Gamma_y = -K_{11}\theta_{,zz} - \lambda_1\dot{\theta} - (\Delta\chi)(H_z^2 - H_x^2)\theta - (v_{x,z}' + v_{y0,z}\varphi)(\lambda_1 + \lambda_2)/2 = 0 \tag{6}$$

$$\Gamma_z = K_{22}\varphi_{,zz} + \lambda_1\dot{\varphi} + (\lambda_2 - \lambda_1)v_{y0,z}\theta/2 + \varphi(H_y^2 - H_x^2)(\Delta\chi) = 0 \tag{7}$$

$$\sigma_{zx} = \mu_3\dot{\theta} + \eta_1 v_{x,z}' + \eta_2 v_{y0,z}\varphi = a \tag{8}$$

$$\mu_4 v_{y,zz}'/2 - \rho g_y \beta T' = 0 \tag{9}$$

$$p_{,z}' + \rho g_z \beta T' = 0 \tag{10}$$

$$k_1 T_{,zz}' + [\mu_4 v_{y0,z} v_{y,z}'] = \rho C\dot{T}' \tag{11}$$

where Γ is the total torque exerted on the director, σ_{zx} the shear stress in the plane xz normal to the yz plane in which convection occurs, K_{ii} the curvature elastic constants, μ_3, μ_6, $\lambda_1 = \mu_2 - \mu_3$, $\lambda_2 = \mu_5 - \mu_6$, $\eta_1 = (\mu_3 + \mu_4 + \mu_6)/2$, $\eta_2 = (\mu_3 + \mu_6)/2$ viscosity coefficients, C the specific heat, $\Delta\chi$ the diamagnetic susceptibility anisotropy, $\dot{\theta} = \partial\theta/\partial t$, etc. and a a function of time. A magnetic field $\mathbf{H} = (H_x, H_y, H_z)$ is included *such that at a given time only one component is nonzero (i.e. when the field acts it does so along x or along y or along z but not along any general direction)*. In Eqs. (6) and (7) terms such as $\Delta\chi(H_z^2 - H_x^2)$, $\Delta\chi(H_y^2 - H_x^2)$ have been written only for economy of expression and to avoid writing different equations for the cases $H_x \neq 0$, $H_y \neq 0$ and $H_z \neq 0$; inertial effects are also ignored.

Equations (6)–(11) are solved subject to the boundary condition

$$(\theta, \varphi, v_x', v_y', T', p')(\pm d/2) = 0 \tag{12}$$

at time t. This implies strong director anchoring at the boundaries. HI threshold is sought by ignoring time dependence. Then a becomes constant. As can

be seen θ, φ and v_x' are determined by Eqs. (6)–(8) while v_y', T' and p' are determined by Eqs. (9)–(11). If, as in Eq. (2) the term [ ] in Eq. (11) is ignored then Eqs. (9)–(12) reduce to

$$v_y' = T' = p' = 0 \tag{13}$$

Thus in a first approximation v_{y0}, T_0 and p_0 can be assumed to be unaltered by the perturbations. Eqs. (6)–(8) support two distinct modes:

Mode 1: θ,φ even; v_x' odd ($a \neq 0$; no net transverse flow)
Mode 2: θ,φ odd; v_x' even ($a \neq 0$; net transverse flow).

The possibility of occurrence of one or both of these modes will be analyzed below separately for MBBA and for HBAB.

3. MBBA ($|\lambda_1| < \lambda_2$)

The HI mechanism for MBBA is well understood[1,3,7] and is given below only for completeness. As is clear from Eq. (5) shear rate is not constant in the sample. Analysis is easier with a variable $\xi = 2z/d$. Then

$$v_{y0}(\xi) = \overline{G}d^3(\xi^3 - \xi)/8;$$

$$v_{y0,\xi} = S(\xi) = \overline{G}d^3(3\xi^2 - 1)/8;$$

$$S(\xi) > 0 \quad \text{for} \quad -1 < \xi < -\frac{1}{\sqrt{3}}; \qquad \frac{1}{\sqrt{3}} < \xi < 1$$

$$S(\xi) < 0 \quad \text{for} \quad -\frac{1}{\sqrt{3}} < \xi < \frac{1}{\sqrt{3}}. \tag{14}$$

There are thus regions in the sample where shear rate has opposite sign. However analysis for one sign of $S(\xi)$ leads to conclusions which are equally valid in all other regions of the sample (except perhaps close to the boundaries if boundary conditions are explicitly taken into account). Thus attention is confined to the case $S(\xi) > 0$.

A. As in Ref. 2, $v_x' = 0$; Eq. (8) is ignored. Mode 1 and Mode 2 can be treated on the same footing. A fluctuation $\theta \sim \theta_1 \cos q\xi$, $\theta_1 > 0$ brings into existence a torque $\Gamma_z^{(\theta)} \sim \theta S(\xi) > 0$ (Eq. 7) which causes a twist $\varphi \sim \phi_1 \cos q\xi$, $\phi_1 > 0$. Torque $\Gamma_y^{(\phi)} \sim (\lambda_1 + \lambda_2)S(\xi)\varphi < 0$ created by φ (Eq. 6) further enhances the original θ perturbation, completing the familiar positive feedback mechanism. The existence of stabilizing elastic

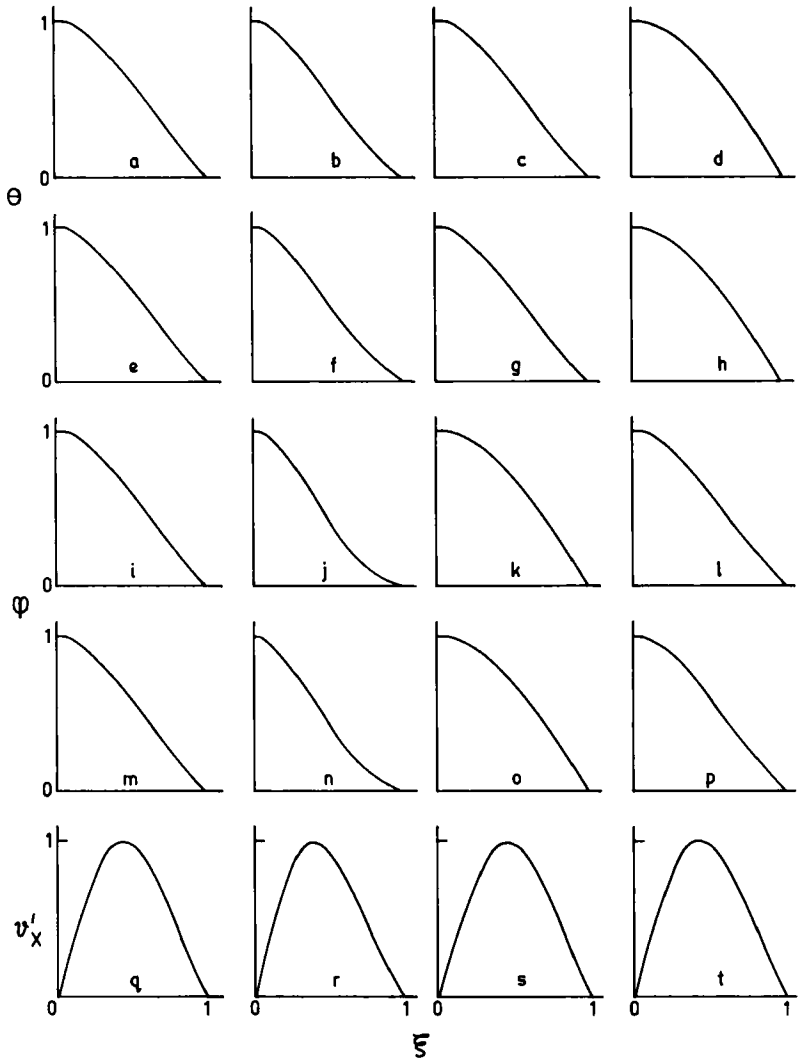

FIGURE 2 Profiles of Mode 1 fluctuations at HI threshold for MBBA. d = 1 mm. Magnetic field in G. ΔT value in parentheses in degree centigrade. Exact calculation. No field (0.52) (a) θ (i) φ (q) ν'_x. H_x = 90 (1.53) (b) θ (f) φ (r) ν'_x. H_y = 50 (0.11) (c) θ (k) φ (s) ν'_x. H_z = 70 (0.1) (d) θ (l) φ (t) ν'_x. Calculation as in Ref. 2, ignoring ν'_x. No field (0.67) (e) θ (m) φ H_x = 90 (2.01) (f) θ (n) φ H_y = 50 (0.14) (g) θ (o) φ H_z = 70 (0.14) (h) θ (p) φ.

torques $\Gamma_y^{el} \sim K_{11}q^2\theta > 0$ (Eq. 6) and $\Gamma_z^{el} \sim -K_{22}q^2\varphi < 0$ (Eq. 7) implies a nonzero threshold. Profiles of perturbations θ and φ are shown in Figure 2 and will be discussed again in Section 3B.

Eqs. (6)–(8) with Eq. (12) have been solved numerically by orthogonal collocation[8] with Legendre polynomials of order 24 and also by series solution technique. Following Ref. 2 one can show that threshold is determined by the critical value G_c of a dimensionless number G:

$$G_c = \left[\frac{\lambda_2^2 - \lambda_1^2}{K_{11}K_{22}}\right]^{1/2} \frac{\rho g \beta}{96\mu_4}[(\Delta T)_c d^3 \cos \psi] = 3.81 \tag{15}$$

With values for MBBA parameters from Table I,

$$E_c = (\Delta T)_c d^3 \cos \psi \simeq 0.67 \times 10^{-3} \text{ cgs} \tag{16}$$

in fair agreement with the experimental value of Ref. 2:

$$E = (\Delta T)_c d^3 \cos \psi \simeq 0.5 \times 10^{-3} \text{ cgs} \tag{17}$$

Both numerical techniques lead to the same critical value 3.81 of G at threshold.

B. Exact analysis: $v_x' \neq 0$: This follows subsection A except for a few differences. Since v_x' is not ignored, Eqs. (6) and (8) can be combined. This shows that presence of v_x' can enhance $\Gamma_y^{(\phi)}$ by a factor $(\eta_1 - \eta_2)/\eta_1 \simeq 1.68$ for MBBA. For Mode 1, perturbations θ, φ and v_x' are scaled by a so that when one speaks of a fluctuation $\theta > 0$ one is actually talking of $\theta/a > 0$. Also, for Mode 1 there exists a constant additional torque $\Gamma_y^a \sim -(\lambda_1 + \lambda_2)/\eta_1$ due to the shear a in the xz plane. Clearly, $\Gamma_y^a < 0$ goes toward a further enhancement of the original θ fluctuation. Computation of threshold is more convenient with orthogonal collocation than with the series solution technique. The Mode 1 threshold is given by

$$\begin{aligned} G_{EC} &= G_c[(\eta_1 - \eta_2)/\eta_1]^{1/2} = 3.81 \\ E_E &= (\Delta T)_c d^3 \cos \psi \approx 0.52 \times 10^{-3} \text{ cgs} \end{aligned} \tag{18}$$

in very close agreement with the experimental result in Eq. (17) of Ref. 2.

As can be seen E_E (Eq. 18) is less than E_c (Eq. 16) by nearly 23%. This decrease can be simply understood by studying Eqs. (6) and (7) for the field-free case. Ignoring v_x', putting $(\theta, \varphi) \sim (\theta_0, \varphi_0) \cos \pi z/d$ and re-

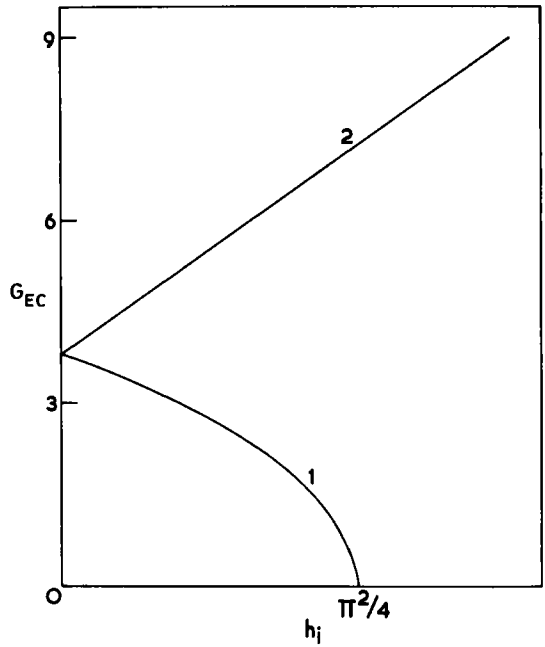

FIGURE 3 MBBA. Variation of HI threshold for Mode 1 with magnetic field. Plot of critical value G_{EC} of the dimensionless number G vs h_i the dimensionless parameter which measures the relative effects of magnetic field and elastic force. (1) G_{EC} vs $h_2 = (\Delta\chi)H_y^2 d^2/4K_{22}$ or G_{EC} vs $h_3 = (\Delta\chi)H_z^2 d^2/4K_{11}$. (2) G_{EC} vs $h_1 = (\Delta\chi)H_x^2 d^2/4(K_{11}K_{22})^{1/2}$ Calculations for $d = 1$ mm. But there is good scaling due to the small value of $\lambda_1 + \lambda_2$.

placing $v_{y0,z}$ by its average value near the sample center $\sim \overline{G}d^2 \sim (\Delta T)d \cos\psi$ the threshold condition becomes

$$(\Delta T)_c^2 d^6 \cos^2\psi = C = \text{constant} \tag{19}$$

where C depends on material parameters. Eq. (19) expresses the fact that the threshold $(\Delta T)_C$ for given d and ψ has the same magnitude regardless of whether the lower plate is hotter or cooler than the upper plate. When secondary flow is included and a ignored for simplicity Eq. (19) gets transformed into

$$[(\Delta T)_c^2 d^6 \cos^2\psi](\eta_1 - \eta_2)/\eta_1 = C \tag{20}$$

showing that the threshold value $(\Delta T)_c$ for given d and ψ gets reduced by a factor $[\eta_1(\eta_1 - \eta_2)]^{1/2}$ as compared to Eq. (19); this corresponds to the decrease mentioned above. The power half results mainly because v_x' enhances Γ_y^ϕ but not Γ_z^θ. Another way of looking at this is from dimensions: shear rate $(\text{Time})^{-1} \sim (\text{Torque per unit area per unit mass})^{1/2}$.

Variation of Mode 1 threshold with magnetic field is shown in Figure 3 and is obvious. Plotting G_{EC} vs the parameter $(\Delta\chi)H^2d^2/K$ yields the same curve for destabilizing H_y or H_z field showing that Eqs. (6)–(8) are scaled. There is very little change in the curves of Figure 3 when d is varied between 0.3 mm and 1 cm. This shows that there is perfect scaling in spite of the additional term $\Gamma_y^{(a)}$ in Eq. (6). This is mainly because this term which is proportional to $(\lambda_1 + \lambda_2)$ is very small compared to the other terms. The decrease of threshold to zero when a destabilizing H_y or H_z field approaches the Freedericksz value is reminiscent of similar calculations[16] on HI threshold for shear flow. The curve in Figure 3 which shows a threshold increase with H_z may not be valid for sufficiently thick samples in which convective instability may be more favorable. A discussion of this falls outside the scope of the present communication.

Profiles of fluctuations θ, φ, v_x' at Mode 1 threshold are shown in Figure 2. At threshold the profiles can be calculated to within a multiplicative constant. All profiles have been presented in the range $0 \leqslant \xi \leqslant 1$ by normalizing with respect to the extremum value of the perturbation

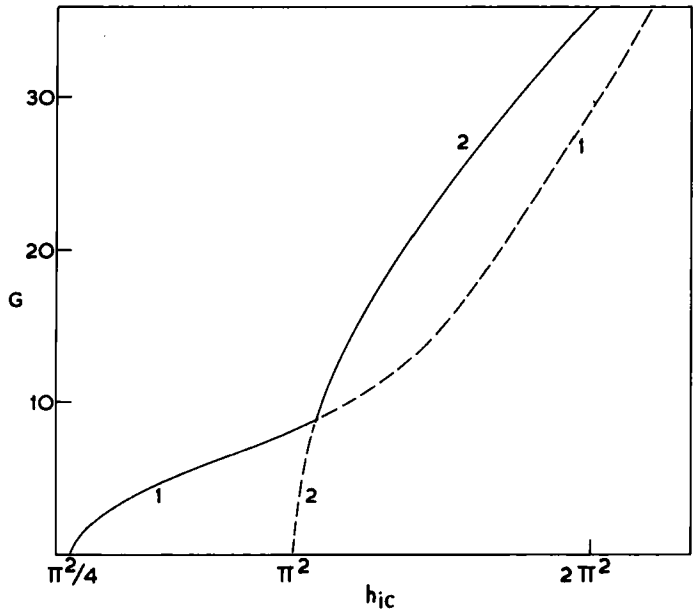

FIGURE 4 HBAB. Variation of G vs h_{ic} · G is a measure of temperature difference ΔT between the plates, h_{ic} is a measure of the critical value H_{yc} or H_{zc} of destabilizing H_y or H_z field necessary to produce HI. The same curve describes effect of H_y or H_z. Threshold exists for $h_{ic} > \pi^2/4$ which is the Freedericksz limit. (1) Mode 1. G vs $h_{2c} = (\Delta\chi)H_{yc}^2d^2/4K_{22}$ or G vs $h_{3c} = (\Delta\chi)H_{zc}^2d^2/4K_{11}$ (2) Mode 2. G vs h_{2c} or h_{3c}. For $G \geqslant 10$, Mode 2 is more favorable than Mode 1. Calculations for $d = 1$ mm. There is good scaling for curve 1 since $\lambda_1 + \lambda_2$ is very small.

occurring in this range. The θ and φ profiles are almost identical for the exact calculation and for the case where v_x' is ignored. Thus the decrease in threshold due to the effect of v_x' seems to be due to an increase of coupling between flow and orientation and not due to any change in the shape of fluctuations. A stabilizing field H_x suppresses θ and φ but enhances v_x' in the bulk of the sample. A field $H_y(H_z)$ enhances $\varphi(\theta)$, diminishes v_x', but leaves $\theta(\varphi)$ unchanged.

So far no mention has been made of Mode 2 for MBBA. This is due to its threshold being higher than the Mode 1 threshold with or without an external magnetic field. The field-free Mode 2 threshold is given by $G_c = 27.2$—nearly seven times the Mode 1 threshold. Thus Mode 2 is of no physical significance for MBBA.

4. HBAB ($|\lambda_1| > \lambda_2$)

Analysis on the same lines as for MBBA shows that, the torque $\Gamma_y^{(\varphi)}$ being > 0, shear stabilizes director orientation against homogeneous perturbations. However for the case in which a small ΔT stabilizes director orientation through free convection, a destabilizing H_y or H_z field greater than the corresponding Freedericksz value H_{Fy} or H_{Fz} can create HI (Figure 4). This is reminiscent of similar results for shear flow HI in HBAB.[17] It should be noted that G for HBAB is written by interchanging λ_1 and λ_2 in Eq. (15). For small ΔT the field threshold for Mode 2 is twice that of Mode 1 and thus Mode 1 is more favorable than Mode 2. This can be understood by analyzing one of the torque equations, *e.g.* Eq. (6) for field H_z near the hydrostatic limit with $\Delta T \approx 0$:

$$\theta_{,zz} + q_z^2\theta = 0; \qquad q_z^2 = (\Delta\chi)H_z^2/K_{11} \tag{21}$$

Eq. (21) can have even or odd solutions. The lowest even and odd harmonics which satisfy Eq. (12) can be written as

$$\theta_E = \theta_{0E} \cos q_{zE}z, \qquad \theta_0 = \theta_{00} \sin q_{z0}z \tag{22}$$

with $q_{zE} = \pi/d$ and $q_{z0} = 2\pi/d$ as threshold conditions. Obviously $q_{zE} = \pi/d$ gives the familiar Freedericksz threshold H_E for an even θ distortion which corresponds to Mode 1, while $q_{z0} = 2\pi/d$ gives the threshold $H_0 = 2H_E$ for an odd θ distortion corresponding to Mode 2 (see end of Section 2 for a definition of modes). Thus for sufficiently small ΔT, Mode 1 is more favorable than Mode 2; the elastic energy associated with Mode 1 distortion is about four times less than that associated with

Mode 2. But for destabilizing fields $>2H_{Fy}$ or $2H_{Fz}$ Mode 2 (curve 2) is more favorable than Mode 1. To understand this crossover from Mode 1 to Mode 2 for field H_y, Eqs. (6) and (7) are written including the effect of v_x' from Eq. (8):

$$K_{11}\theta_{,zz} + v_{y0,z}\varphi(\lambda_1 + \lambda_2)(\eta_1 - \eta_2)/2\eta_1 = 0 \tag{23}$$

$$K_{22}\varphi_{,zz} + (\Delta\chi)H_y^2\varphi + (\lambda_2 - \lambda_1)v_{y0,z}\theta/2 = 0 \tag{24}$$

For simplicity a is ignored, boundary conditions on v_x' are also not considered and $v_{y0,z}$ is replaced by its average value near the sample center, viz., $-\overline{G}d^2/6$. For Mode 1 with $(\theta, \varphi) = (\theta_0, \varphi_0) \cos \pi z/d$ the threshold condition is

$$h_{EC} = \pi^2/4 + X(\Delta T)^2 \cos^2 \psi = (\Delta\chi)H_{yE}^2 d^2/4K_{22} \tag{25}$$

with $X = \rho^2\beta^2 d^6 g^2(\lambda_1^2 - \lambda_2^2)/[5184\, K_{11}K_{22}\pi^2\mu_4(\mu_3 + \mu_4 + \mu_6)] > 0$. The threshold condition for Mode 2, with $(\theta, \varphi) = (\theta_0, \varphi_0) \sin 2\pi z/d$ becomes

$$h_{0c} = \pi^2 + X(\Delta T)^2(\cos^2 \psi)/4 = (\Delta\chi)H_{y0}^2 d^2/4K_{22} \tag{26}$$

This shows that when ΔT increases from zero the field H_y necessary to produce Mode 1 or Mode 2 increases from the corresponding static value $h_{Ec} = \pi^2/4$ or $h_{0c} = \pi^2$. For small enough ΔT, $h_{0c} > h_{Ec}$ so that Mode 1 is more favorable than Mode 2 as already indicated. However the variation $h_{0c} - \pi^2$ of h_{0c} (Mode 2) from its static threshold value of π^2 is four times less than the corresponding variation $h_{Ec} - \pi^2/4$ of h_{Ec} (Mode 1). This can also be seen from Eqs. (25) and (26) by differentiation

$$d h_{Ec}/d(\Delta T) = 2X(\Delta T) \cos \psi = 4dh_{0c}/d(\Delta T) \tag{27}$$

Thus as (ΔT) increases from zero both h_{Ec} and h_{0c} increase but the former increases four times faster than the latter. There thus exists a $(\Delta T)_0$ such that $h_{Ec} = h_{0c}$ i.e. both modes are equally favorable. From Eqs. (25) and (26)

$$(\Delta T)_0 \cos \psi = \pi/X^{1/2} \tag{28}$$

for a field H_y such that

$$h_{Ec} = h_{0c} = 5\pi^2/4 \tag{29}$$

Exactly the same analysis applies for a field H_z. Needless to say, for $\Delta T > (\Delta T)_0$ Mode 2 is more favorable than Mode 1. Thus unless a convective instability occurs for $\Delta T \leqslant (\Delta T)_0$ it should be possible to observe a crossover to Mode 2 which is associated with net transverse flow when a destablilizing magnetic field of sufficient strength is used. For HBAB,

with $d = 1$ mm, Eqs. (28) and (29) yield $(\Delta T)_0 \cos \psi \approx 1.5°C$, $H_{yc} \approx 180$ G or $H_{zc} \approx 240$ G while the exact calculation (Figure 4) gives $(\Delta T)_0 \cos \psi \approx 1.8°C$, $H_{yc} \approx 165$ G or $H_{zc} \approx 215$ G. This seems similar to the possibility envisaged earlier, of observing an unfavorable Mode in plane Poiseuille flow instabilities of HBAB.[16,17] The crossover from Mode 1 to Mode 2 can be shown to occur for HBAB using the simplified model of Ref. 2. The only difference will be that the value of $(\Delta T)_0 \cos \psi$ will be higher by a factor $[(\eta_1 - \eta_2)/\eta_1]^{1/2} \approx 1.25$.

Figures 5 and 6 contain plots of perturbations at HI threshold for HBAB. For Mode 1, when ΔT increases and H_{yc} or H_{zc} increases from its Freedericksz value, the effective wave vector of distortion at threshold (EWV) increases for both θ and φ. While H_z does not perceptibly affect v_x' an increasing H_y diminishes v_x' in the bulk. For Mode 2, when ΔT increases H_{yc} (H_{zc}) increases EWV of $\theta(\varphi)$ and diminishes the amplitude of $\varphi(\theta)$ in the bulk. With increasing ΔT, H_{yc} or H_{zc} increases net secondary flow but EWV of v_x' is larger for H_y than for H_z. The profiles of θ and φ with v_x' ignored are fairly similar to those obtained from the exact calculation which again suggests that the crossover from Mode 1 to Mode 2 can occur even when v_x' is zero. Comparison of Mode 1 and Mode 2 profiles suggests a possible explanation of this crossover. At small ΔT, EWV of Mode 1 is smaller than that of Mode 2 for both θ and φ. Since critical field ~ EWV, the field threshold for Mode 1 is less than that for Mode 2. When ΔT increases, in the case of Mode 1 EWV increases for both θ and φ while in the case of Mode 2 EWV increases for only one perturbation. This could explain the rapid increase of the Mode 1 field threshold as compared to the increase of Mode 2 field threshold as ΔT increases and a consequent crossover from Mode 1 to Mode 2 at sufficiently high ΔT. It should however be stressed that this explanation is tentative; it is difficult to calculate EWV easily because shear rate is not constant in this problem.

The curves in Figure 4 also exhibit scaling. While this is not surprising for Mode 2, it can be understood for Mode 1 also because $\lambda_1 + \lambda_2$ is very small for HBAB. If $\lambda_1 + \lambda_2$ is very large a lack of scaling may be manifest for Mode 1 due to the term $\Gamma_y^{(a)}$. It is tempting to wonder whether this lack of scaling of the threshold curves will manifest in experiments on materials such as CBOOA[18] or 8CB[19] near the smectic–nematic transition where $\alpha_3 = -(\lambda_1 + \lambda_2)/2$ becomes positive and even diverges.

In conclusion one must point out certain limitations of the present model. Improvements on these calculations would involve including effects of (i) finite anchoring energy of director orientation at the boundaries, (ii) finite sample width (along x), (iii) boundary layers, especially in thick samples, (iv) nonlinear perturbations.

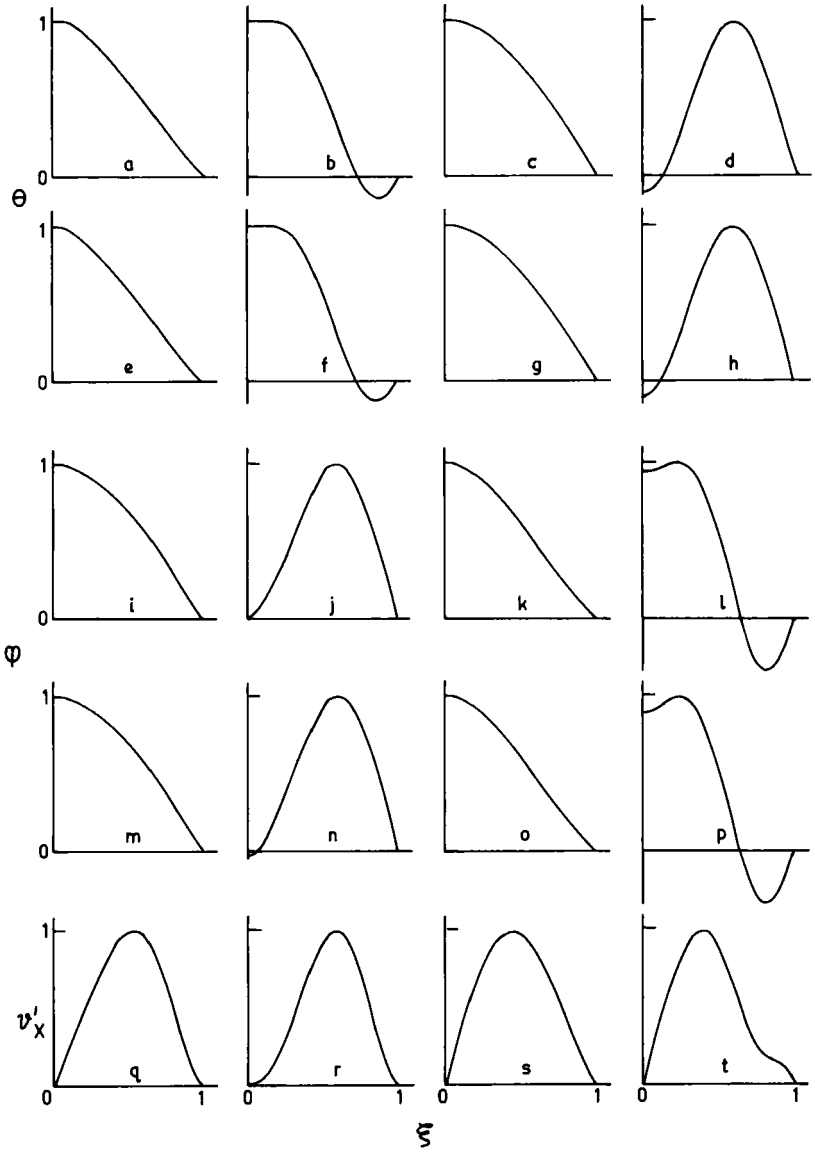

FIGURE 5 Profiles of Mode 1 fluctuations at HI threshold for HBAB. d = 1 mm. Magnetic field in G. ΔT value in parentheses. Exact calculation H_y = 80 (0.08) (a) θ (i) φ (q) ν'_x. H_y = 200 (3.58) (b) θ (j) φ (r) ν'_x H_z = 106 (0.03) (c) θ (k) φ (s) ν'_x. H_z = 280 (4.69) (d) θ (1) φ (t) ν'_x. Calculation as in Ref. 2, ignoring ν'_x. H_y = 80 (0.105) (e) θ (m) φ; H_y = 200 (4.44) (f) θ (n) φ; H_z = 106 (0.04) (g) θ (o) φ; H_z = 280 (5.79) (h) θ (p) φ.

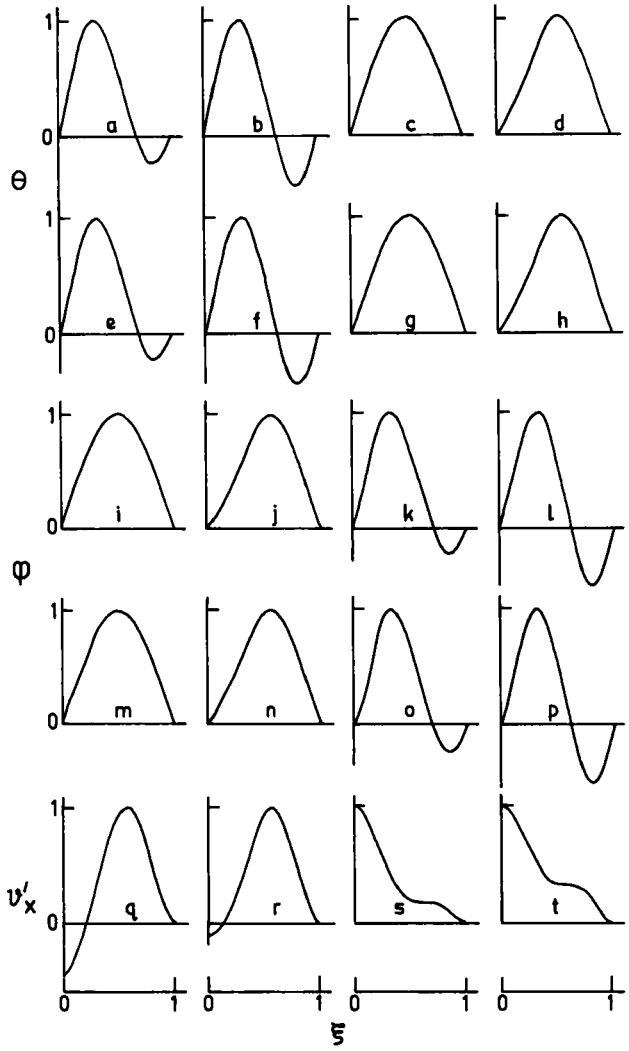

FIGURE 6 Profiles of Mode 2 fluctuations at HI threshold for HBAB. d = 1 mm. Magnetic field in G. ΔT in parantheses. Exact calculation. H_y = 160 (0.67) (a) θ (i) φ (q) ν'_x; H_y = 200 (5.32) (b) θ (j) φ (r) ν'_x; H_z = 212 (0.45) (c) θ (k) φ (s) ν'_x; H_z = 280 (6.2) (d) θ (l) φ (t) ν'_x; Calculations as in Ref. 2, ignoring ν'_x. H_y = 160 (0.84) (e) θ (m) φ; H_y = 200 (6.64) (f) θ (n) φ; H_z = 212 (0.57) (g) θ (o) φ; H_z = 280 (7.74) (h) θ (p) φ.

Acknowledgments

The author thanks Prfoessor S. Chandrasekhar for encouragement during the course of this work. He also thanks the referee for helpful comments.

References

1. E. Dubois-Violette, G. Durand, E. Guyon, P. Manneville and P. Pieranski, in *Solid State Physics, Supplement 14,* (Academic, 1978) 147–208.
2. D. Horn, E. Guyon and P. Pieranski, *Rev. de Phys. Appl.*, **11**, 139 (1976).
3. P. Pieranski and E. Guyon, *Solid State Commun.*, **13**, 435 (1973).
4. E. Guyon, P. Pieranski and M. Boix, *J. de Phys.*, **39**, 99 (1978).
5. F. M. Leslie, *Arch. Ration. Mech. Anal.*, **28**, 265 (1978).
6. L. D. Landau and E. M. Lifshitz, *Fluids Mechanics* (Pergamon, 1966).
7. P. Manneville and E. Dubois-Violette, *J. de Phys.*, **37**, 285 (1976).
8. B. A. Finlayson, *The Method of Weighted Residuals and Variational Principles* (Academic, 1972).
9. M. J. Stephen and J. P. Straley, *Rev. Mod. Phys.*, **46**, 617 (1974).
10. Ch. Gahwiller, *Phys. Lett.*, **36A(4)**, 311 (1971).
11. Ch. Gahwiller, *Mol. Cryst. Liq. Cryst.*, **20**, 301 (1973).
12. I. Haller, *J. Chem. Phys.*, **57**, 1400 (1972).
13. H. Gasparoux, B. Regaya and J. Prost, *C. R. Hebd. Sean. Acad. Sci. Paris,* **B272**, 1168 (1971).
14. P. E. Cladis, *Phys. Rev. Lett.*, **35**, 48 (1975).
15. P. E. Cladis and S. Torza, *Phys. Rev. Lett.*, **35**, 1283 (1975).
16. U. D. Kini, *Pramana,* **10**, 143 (1978).
17. U. D. Kini, *Pramana,* **15**, 231 (1980).
18. P. Pieranski and E. Guyon, *Commun. Phys.*, **1**, 45 (1976).
19. K. Skarp, T. Carlsson, S. T. Lagerwall and B. Stebler, *Mol. Cryst. Liq. Cryst.*, **59**, 63 (1980).